

## NON-LINEAR OSCILLATIONS OF A SIMPLY-SUPPORTED THIN-WALLED COMPOSITE BEAM

**Sebastián P. Machado**

Grupo Análisis de Sistemas Mecánicos, Universidad Tecnológica Nacional (FRBB), 11 de Abril 461, 8000, Bahía Blanca, Argentina  
smachado@frbb.utn.edu.ar

**Víctor H. Cortínez**

Grupo Análisis de Sistemas Mecánicos, Universidad Tecnológica Nacional (FRBB), 11 de Abril 461, 8000, Bahía Blanca, Argentina  
vcortine@frbb.utn.edu.ar

**Abstract.** *A geometrically non-linear theory is used to study the dynamic behavior of a thin-walled composite beam. The model is based on a small strain and large rotation and displacements theory, which is formulated through the adoption of a higher-order displacement field and takes into account shear flexibility (bending and warping shear). In the analysis of a weakly nonlinear continuous system, the Ritz's method is employed to express the problem in terms of generalized coordinates. Then, perturbation method of multiple scales is applied to the reduced system in order to obtain the equations of amplitude and modulation. In this paper, the non-linear 3D oscillations of a simply-supported beam are examined, considering a cross-section having one symmetry axis. Composite is assumed to be made of symmetric balanced laminates and especially orthotropic laminates. The model, which contains both quadratic and cubic non-linearities, is assumed to be in internal resonance condition. Steady-state solution and their stability are investigated by means of the eigenvalues of the Jacobian matrix. The software XPP-AUTO is used to trace the branches of the equilibrium solutions. The equilibrium solution is governed by the modal coupling and experience a complex behavior composed by saddle-nodde, hopf and double period bifurcations.*

**Keywords:** *Composite, thin-walled beam, non-linear model, dynamic.*

### 1. INTRODUCTION

Thin-walled beam structures made of advanced anisotropic composite materials are increasingly found in the design of the aircraft wing, helicopter blade, axles of vehicles and so on, due to their outstanding engineering properties, such as high strength/stiffness to weight ratios and favorable fatigue characteristics. The interesting possibilities provided by fiber reinforced composite materials can be used to enhance the response characteristics of such structures that operate in complex environmental conditions. We consider the nonlinear response of a simply supported beam to a primary resonant excitation of its first mode. The analysis accounts for a lateral load, modal damping and unidirectional fiber orientation. The second and third natural frequencies are approximately two and three times the first natural frequency, respectively. The flexural-torsional coupling produces a quadratic and cubic nonlinearity in the governing nonlinear partial-differential equation. Because of the quadratic and cubic nonlinearity and the two-to-one and three-to-one ratio of the second and third with the first natural frequencies, the beam exhibits an internal (autoparametric) resonance that couples the first, second and third modes, resulting in energy exchange between them.

For a comprehensive review of nonlinear modal interactions, we refer the reader to Nayfeh and Mook (1979), Nayfeh and Balachandran (1989), and Nayfeh (1996). In this paper, we present a brief review of some of the studies of the response of systems exhibiting two-to-one and three-to-one internal resonances to primary resonant excitations.

Crespo da Silva and Glynn (1978 a and b) developed a non-linear shear-undeformable beam model with a compact cross-section and derived a set of integro-partial-differential equations governing flexural-flexural-torsional motions of inextensional beams, including geometric and inertia nonlinearities. They used these equations and the method of multiple scales to ascertain the importance of the geometric terms (Crespo da Silva and Glynn, 1978b); they found that they cannot be neglected for the lower modes, especially the first mode. Luongo *et al.* (1989) and Crespo da Silva *et al.* (1994) analyzed shear and axially undeformable beams. In (Luongo *et al.*, 1989) flexural-torsional free motions are studied for a cantilever beam, having close bending and torsional frequencies; although beams with non-compact cross-section are considered, the warping effects are neglected. In these articles a non-linear one-dimensional polar model of compact beam is derived, capable of studying interactions between flexural and torsional motions occurring in beam-like structures in several internal resonance conditions. In spite of the practical interest and future potential of the composite beam structures, particularly in the context of aerospace and mechanical applications, there are not investigations about the nonlinear dynamic response of thin-walled composite beams.

In this paper, a geometrically non-linear beam model is developed to study three dimensional large amplitude oscillations. The model is valid for symmetric balanced laminates and incorporates, in a full form, the effects of shear flexibility. In order to perform the nonlinear dynamic analysis the Galerkin procedure, is used to obtain a discrete form of the equations of motion. Multiple time scale method (Nayfeh, 1973) is used to obtain modulation-phase equations and the reconstitution method first proposed in (Nayfeh, 1985) is adopted to return to the true time domain. Steady-state solutions and their stability are studied by using the model proposed.

## 2. KINEMATICS

A straight thin-walled composite beam with an arbitrary cross-section is considered (Fig. 1). The points of the structural member are referred to a Cartesian co-ordinate system  $(x, \bar{y}, \bar{z})$ , where the  $x$ -axis is parallel to the longitudinal axis of the beam while  $\bar{y}$  and  $\bar{z}$  are the principal axes of the cross-section. The axes  $y$  and  $z$  are parallel to the principal ones but having their origin at the shear center (defined according to Vlasov's theory of isotropic beams). The co-ordinates corresponding to points lying on the middle line are denoted as  $Y$  and  $Z$  (or  $\bar{Y}$  and  $\bar{Z}$ ). In addition, a circumferential co-ordinate  $s$  and a normal co-ordinate  $n$  are introduced on the middle contour of the cross-section.

$$\bar{y}(s, n) = \bar{Y}(s) - n \frac{dZ}{ds}, \quad \bar{z}(s, n) = \bar{Z}(s) + n \frac{dY}{ds} \quad (1)$$

$$y(s, n) = Y(s) - n \frac{dZ}{ds}, \quad z(s, n) = Z(s) + n \frac{dY}{ds} \quad (2)$$

On the other hand,  $y_0$  and  $z_0$  are the centroidal co-ordinates measured with respect to the shear center.

$$\begin{aligned} \bar{y}(s, n) &= y(s, n) - y_0 \\ \bar{z}(s, n) &= z(s, n) - z_0 \end{aligned} \quad (3)$$

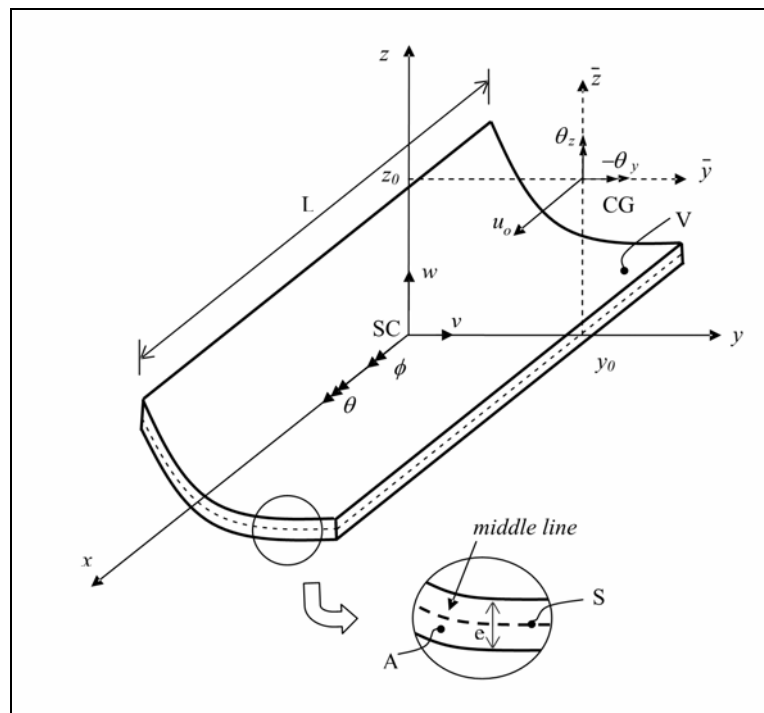


Figure 1. Co-ordinate system of the cross-section and notation for displacement measures.

The present structural model is based on the following assumptions:

- 1) The cross-section contour is rigid in its own plane.
- 2) The warping distribution is assumed to be given by the Saint-Venant function for isotropic beams.
- 3) Flexural rotations (about the  $\bar{y}$  and  $\bar{z}$  axes) are assumed to be moderate, while the twist  $\phi$  of the cross-section can be arbitrarily large.
- 4) Shell force and moment resultants corresponding to the circumferential stress  $\sigma_{ss}$  and the force resultant corresponding to  $\gamma_{ns}$  are neglected.
- 5) The curvature at any point of the shell is neglected.
- 6) Twisting linear curvature of the shell is expressed according to the classical plate theory.
- 7) The laminate stacking sequence is assumed to be symmetric and balanced (Barbero, 1999).

According to these hypotheses the displacement field is assumed to be in the following form

$$\begin{aligned}
 u_x &= u_o - \bar{y}(\theta_z \cos \phi - \theta_y \sin \phi) - \bar{z}(\theta_y \cos \phi - \theta_z \sin \phi) + \omega \left[ \theta - \frac{1}{2}(\theta_y' \theta_z - \theta_y \theta_z') \right] + (\theta_z z_o - \theta_y y_o) \sin \phi \\
 u_y &= v - z \sin \phi - y(1 - \cos \phi) - \frac{1}{2}(\theta_z^2 \bar{y} + \theta_z \theta_y \bar{z}) \\
 u_z &= w + y \sin \phi - z(1 - \cos \phi) - \frac{1}{2}(\theta_y^2 \bar{z} + \theta_z \theta_y \bar{y})
 \end{aligned} \tag{4}$$

This expression is a generalization of others previously proposed in the literature as explained for Machado *et al.* (2005). In the above expressions  $\phi$ ,  $\theta_y$  and  $\theta_z$  are measures of the rotations about the shear center axis,  $\bar{y}$  and  $\bar{z}$  axes, respectively;  $\theta$  represents the warping variable of the cross-section. Furthermore the superscript ‘prime’ denotes derivation with respect to the variable  $x$ .

The components of the Green’s strain tensor which incorporates the large displacement are obtained as explained in (Machado *et al.* 2005).

### 3. VARIATIONAL FORMULATION

Taking into account the adopted assumptions, the principle of virtual work for a composite shell may be expressed in the form:

$$\begin{aligned}
 & \iint (N_{xx} \delta \varepsilon_{xx}^{(0)} + M_{xx} \delta \kappa_{xx}^{(l)} + N_{xs} \delta \gamma_{xs}^{(0)} + M_{xs} \delta \kappa_{xs}^{(l)} + N_{xn} \delta \gamma_{xn}^{(0)}) ds dx \\
 & - \iiint \rho (\ddot{u}_x \delta u_x + \ddot{u}_y \delta u_y + \ddot{u}_z \delta u_z) ds dn dx \\
 & - \iint (\bar{q}_x \delta \bar{u}_x + \bar{q}_y \delta \bar{u}_y + \bar{q}_z \delta \bar{u}_z) ds dx - \iint (\bar{p}_x \delta u_x + \bar{p}_y \delta u_y + \bar{p}_z \delta u_z) \Big|_{x=0} ds dn \\
 & - \iint (\bar{p}_x \delta u_x + \bar{p}_y \delta u_y + \bar{p}_z \delta u_z) \Big|_{x=L} ds dn - \iiint (\bar{f}_x \delta u_x + \bar{f}_y \delta u_y + \bar{f}_z \delta u_z) ds dn dx = 0
 \end{aligned} \tag{5}$$

where  $N_{xx}$ ,  $N_{xs}$ ,  $M_{xx}$ ,  $M_{xs}$  and  $N_{xn}$  are the shell stress resultants. The beam is subjected to wall surface tractions  $\bar{q}_x$ ,  $\bar{q}_y$  and  $\bar{q}_z$  specified per unit area of the undeformed middle surface and acting along the  $x$ ,  $y$  and  $z$  directions, respectively. Similarly,  $\bar{p}_x$ ,  $\bar{p}_y$  and  $\bar{p}_z$  are the end tractions per unit area of the undeformed cross-section specified at  $x = 0$  and  $x = L$ , where  $L$  is the undeformed length of the beam. Besides  $\bar{f}_x$ ,  $\bar{f}_y$  and  $\bar{f}_z$  are the body forces per unit of volume. Finally, denoting  $\bar{u}_x$ ,  $\bar{u}_y$  and  $\bar{u}_z$  as displacements at the middle line.

### 4. CONSTITUTIVE EQUATIONS

The constitutive equations of symmetrically balanced laminates may be expressed in the terms of shell stress resultants in the following form (Barbero, 1999):

$$\begin{Bmatrix} N_{xx} \\ N_{xs} \\ N_{xn} \\ M_{xx} \\ M_{xs} \end{Bmatrix} = \begin{bmatrix} \bar{A}_{11} & 0 & 0 & 0 & 0 \\ 0 & \bar{A}_{66} & 0 & 0 & 0 \\ 0 & 0 & \bar{A}_{55}^{(H)} & 0 & 0 \\ 0 & 0 & 0 & \bar{D}_{11} & 0 \\ 0 & 0 & 0 & 0 & \bar{D}_{66} \end{bmatrix} \begin{Bmatrix} \varepsilon_{xx}^{(0)} \\ \gamma_{xs}^{(0)} \\ \gamma_{xn}^{(0)} \\ \kappa_{xx}^{(l)} \\ \kappa_{xs}^{(l)} \end{Bmatrix} \tag{6}$$

with

$$\begin{aligned}
 \bar{A}_{11} &= A_{11} - \frac{A_{12}^2}{A_{22}}, & \bar{A}_{66} &= A_{66} - \frac{A_{26}^2}{A_{22}}, & \bar{A}_{55}^{(H)} &= A_{55}^{(H)} - \frac{(A_{45}^{(H)})^2}{A_{44}^{(H)}} \\
 \bar{D}_{11} &= D_{11} - \frac{D_{12}^2}{D_{22}}, & \bar{D}_{66} &= D_{66} - \frac{D_{26}^2}{D_{22}}
 \end{aligned} \tag{7}$$

where  $A_{ij}$ ,  $D_{ij}$  and  $A_{ij}^{(H)}$  are plate stiffness coefficients defined according to the lamination theory presented by Barbero (1999). The coefficient  $\overline{D}_{16}$  has been neglected because of its low value for the considered laminate stacking sequence.

## 5. PRINCIPLE OF VIRTUAL WORK FOR THIN-WALLED BEAMS

Substituting the kinematics expressions and the constitutive equations into (5) and integrating with respect to  $s$ , one obtains the one-dimensional expression for the virtual work equation given by:

$$L_M + L_K + L_P = 0 \quad (8)$$

where  $L_M$ ,  $L_K$  and  $L_P$  represent the virtual work contributions due to the inertial, internal and external forces, respectively.

$$L_M = \int_0^L \rho \left[ A \frac{\partial^2 u_0}{\partial t^2} \delta u_0 + I_z \frac{\partial^2 \theta_z}{\partial t^2} \delta \theta_z + I_y \frac{\partial^2 \theta_y}{\partial t^2} \delta \theta_y + C_w \frac{\partial^2 \theta}{\partial t^2} \delta \theta + A \frac{\partial^2}{\partial t^2} (v - z_0 \phi) \delta v \right. \\ \left. + A \frac{\partial^2}{\partial t^2} (w + y_0 \phi) \delta w + \frac{\partial^2}{\partial t^2} (-Az_0 v + Ay_0 w + I_s \phi) \delta \phi \right] dx \quad (9)$$

where  $A$  is the cross-sectional area,  $I_z$  and  $I_y$  are the principal moments of inertia of the cross-section,  $C_w$  is the warping constant,  $I_s$  is the polar moment with respect to the shear center and  $\rho$  is the mean density of the laminate.

$$L_K = \int_0^L \left\{ \delta u'_0 \left[ N + u'_0 N - M_z (\theta'_z \cos \phi + \theta'_y \sin \phi) - M_y (\theta'_y \cos \phi + \theta'_z \sin \phi) - Q_y (\theta_z \cos \phi + \theta_y \sin \phi) \right. \right. \\ \left. \left. - Q_z (\theta_y \cos \phi + \theta_z \sin \phi) \right] + \delta v' (Q_y \cos \phi - Q_z \sin \phi + v' N) + \delta w' (Q_z \cos \phi + Q_y \sin \phi + w' N) \right. \\ \left. + \delta \theta_z \left[ -Q_y (I + u'_0) \cos \phi + Q_z (I + u'_0) \sin \phi + \frac{1}{2} (Q_z y_0 - Q_y z_0) \theta'_y - \frac{1}{2} T_{sv} \theta'_y - \frac{1}{2} B \theta''_y \right] \right. \\ \left. + \delta \theta'_z \left[ -M_z (I + u'_0) \cos \phi + M_y (I + u'_0) \sin \phi + N z_0 \sin \phi + \frac{1}{2} (Q_y z_0 - Q_z y_0) \theta_y + \frac{1}{2} T_{sv} \theta_y + \theta'_z P_{zz} + \theta'_y P_{yz} \right] \right. \\ \left. + \delta \theta_y \left[ -Q_z (I + u'_0) \cos \phi - Q_y (I + u'_0) \sin \phi + \frac{1}{2} (Q_y z_0 - Q_z y_0) \theta'_z + \frac{1}{2} T_{sv} \theta'_z + \frac{1}{2} B \theta''_z \right] \right. \\ \left. + \delta \theta'_y \left[ -M_y (I + u'_0) \cos \phi - M_z (I + u'_0) \sin \phi - N y_0 \sin \phi + \frac{1}{2} (Q_z y_0 - Q_y z_0) \theta_z - \frac{1}{2} T_{sv} \theta_z + \theta'_z P_{yz} + \theta'_y P_{yy} \right] \right. \\ \left. + \delta \phi \left[ M_y ((\theta'_y + \theta'_y u'_0) \sin \phi + (\theta'_z + \theta'_z u'_0) \cos \phi) + M_z ((\theta'_z + \theta'_z u'_0) \sin \phi - (\theta'_y + \theta'_y u'_0) \cos \phi) \right. \right. \\ \left. \left. + Q_y ((\theta_z - v' + \theta_z u'_0) \sin \phi - (\theta_y - w' + \theta_y u'_0) \cos \phi) + N (z_0 \theta'_z - y_0 \theta'_y) \cos \phi \right. \right. \\ \left. \left. + Q_z ((\theta_y - w' + \theta_y u'_0) \sin \phi + (\theta_z - v' + \theta_z u'_0) \cos \phi) \right] + \delta \theta''_z \frac{1}{2} B \theta_y - \delta \theta''_y \frac{1}{2} B \theta_z \right. \\ \left. + \delta \phi' [T_w + T_{sv} + B_l \phi'] + \delta \theta' B - \delta \theta T_w \right\} dx \quad (10)$$

The expressions of  $L_P$  are the same as presented by the authors in [12]; in the same way the 1-D beam forces, in terms of the shell forces, have been defined for Machado *et al.* (2005).

### 5.1. Discrete model

The equations of motion are discretized according to the Galerkin procedure. The independent displacements vector is expressed as a linear combination of given  $x$ -function vectors  $\mathbf{f}_k(x) = \{f_{k1}(x), f_{k2}(x), f_{k3}(x)\}$  and unknown  $t$ -function coefficients  $q_k(t)$ :

$$\mathbf{u}(x, t) = \sum_{k=1}^n q_k(t) \mathbf{f}_k(x) \quad (11)$$

The functions  $\mathbf{f}_k(x)$  are chosen as eigenfunctions of the linearized equations and boundary conditions. Since for a generic cross-section even the linear equations are coupled, all the components of  $\mathbf{f}_k(x)$  are different from zero. By substituting Eqs.(11) into Eq. (8) and vanishing separately terms in  $\delta q_k$ ;  $3n$  ordinary differential equations of motion follow. By limiting the expansion (11) to  $n = 3$  terms (e.g. by assuming a group of three modes with similar wave-length), three non-linear equations of the following type are obtained:

$$\ddot{q}_k + \omega_k^2 q_k = \sum_{i=1}^n \sum_{j=1}^n c_{kij} q_i q_j + \sum_{i=1}^n \sum_{j=1}^n \sum_{m=1}^n c_{kijm} q_i q_j q_m + f_k \quad (k = 1, 2, 3, \dots, n.) \quad (12)$$

where  $\omega_k$  is the  $k$ th linear frequency,  $f_k$  the  $k$ th modal force, and  $c_{kij}$  and  $c_{kijm}$  are coefficients depending on eigenfunctions. In the general case all quadratic and cubic terms appear in each equation of motion.

## 5.2. Amplitude and phase equations for the discrete model

A simply-supported beam with a monosymmetric cross-section, loaded by a concentrated harmonic force applied to the beam's centroid axis acting along the vertical section is considered, see Fig. 2. Using a three-mode discretization, the non-linear flexural–flexural–torsional oscillations are governed by the following three ordinary differential equations:

$$\begin{aligned} \ddot{q}_1 + d_1 \dot{q}_1 + \omega_1^2 q_1 &= c_1 q_1 q_2 + c_2 q_2 q_3 + c_3 q_1^3 + c_4 q_3^3 + c_5 q_1 q_2^2 + c_6 q_1 q_3^2 + c_7 q_3 q_1^2 + c_8 q_3 q_2^2 + c_{19} P \\ \ddot{q}_2 + d_2 \dot{q}_2 + \omega_2^2 q_2 &= c_9 q_1^2 + c_{10} q_2^2 + c_{11} q_3^2 + c_2 q_1 q_3 + c_{12} q_1 q_2 q_3 + c_{13} q_2^3 + c_5 q_2 q_1^2 + c_{14} q_2 q_3^2 \\ \ddot{q}_3 + d_3 \dot{q}_3 + \omega_3^2 q_3 &= c_2 q_1 q_2 + c_{15} q_2 q_3 + c_{16} q_1^3 + c_{17} q_3^3 + c_8 q_1 q_2^2 + c_{18} q_1 q_3^2 + c_6 q_3 q_1^2 + c_{14} q_3 q_2^2 + c_{20} P \end{aligned} \quad (13)$$

where  $q_i$  is the  $i$ th mode amplitude,  $d_i$  are the modal damping coefficients and  $P(t) = p e^{i\Omega t}$  is the load, of frequency  $\Omega$  assumed to be in primary resonance with the  $q_1$ -mode. Moreover, the beam is assumed to be in internal resonance conditions of the kind 2:3:1, so that quadratic, cubic and combination resonances occur.

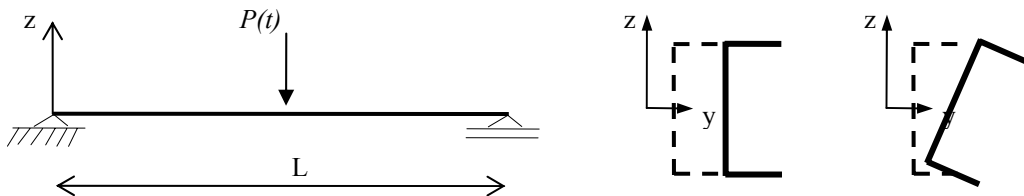


Figure 2. Simply-supported C-beam and midspan section displacements of the fundamentals eigenfunctions.

The method of multiple time scales is employed to study the non-linear equations (13). Since non-linear terms are quadratic and cubic, a second-order expansion is developed. A small parameter  $\varepsilon$  is introduced by ordering the linear damping and load amplitude as  $d_i = \varepsilon^2 \tilde{d}_i$ ,  $p = \varepsilon^3 \tilde{p}$ . Moreover, the displacements  $q_i$  are expanded as:

$$q_i(T_0, T_1, T_2, \varepsilon) = \varepsilon q_i^{(0)}(T_0, T_1, T_2, \varepsilon) + \varepsilon^2 q_i^{(1)}(T_0, T_1, T_2, \varepsilon) + \varepsilon^3 q_i^{(2)}(T_0, T_1, T_2, \varepsilon) \quad (14)$$

where,  $T_0 = t$ ,  $T_1 = \varepsilon t$ ,  $T_2 = \varepsilon^2 t$ .  $T_0$  is a fast scale, on which motions with frequencies of the order of  $\Omega$  occur, while  $T_1$  and  $T_2$  are the slow scales, on which modulations of the amplitudes and phases take place.

Substituting Eq. (14) into Eq. (13) and equating coefficients of like powers of  $\varepsilon$ , the following perturbation equations are obtained:

Order  $\varepsilon$ :

$$D_0^2 q_i^{(0)} + \omega_i^2 q_i^{(0)} = 0, \quad (i = 1, 2, 3) \quad (15)$$

Orden  $\varepsilon^2$  :

$$\begin{aligned}
D_0^2 q_1^{(1)} + \omega_1^2 q_1^{(1)} &= -2D_0 D_1 q_1^{(0)} + c_1 q_1^{(0)} q_2^{(0)} + c_2 q_2^{(0)} q_3^{(0)} \\
D_0^2 q_2^{(1)} + \omega_2^2 q_2^{(1)} &= -2D_0 D_1 q_2^{(0)} + c_9 q_1^{(0)^2} + c_{10} q_2^{(0)^2} + c_2 q_1^{(0)} q_3^{(0)} + c_{11} q_3^{(0)^2} \\
D_0^2 q_3^{(1)} + \omega_3^2 q_3^{(1)} &= -2D_0 D_1 q_3^{(0)} + c_2 q_1^{(0)} q_2^{(0)} + c_{15} q_2^{(0)} q_3^{(0)}
\end{aligned} \tag{16}$$

Orden  $\varepsilon^3$  :

$$\begin{aligned}
D_0^2 q_1^{(2)} + \omega_1^2 q_1^{(2)} &= -d_1 D_0 q_1^{(0)} - 2D_0 D_1 q_1^{(1)} - D_1^2 q_1^{(0)} - 2D_0 D_2 q_1^{(0)} + c_3 q_1^{(0)^3} + c_1 q_1^{(1)} q_2^{(0)} + c_5 q_1^{(0)} q_2^{(0)^2} + c_1 q_1^{(0)} q_2^{(1)} \\
&\quad + c_7 q_1^{(0)^2} q_3^{(0)} + c_8 q_2^{(1)^2} q_3^{(0)} + c_2 q_2^{(1)} q_3^{(0)} + c_6 q_1^{(0)} q_3^{(0)^2} + c_4 q_3^{(0)^3} + c_2 q_2^{(0)} q_3^{(1)} + c_{19} p e^{i\Omega T_0} \\
D_0^2 q_2^{(2)} + \omega_2^2 q_2^{(2)} &= -d_2 D_0 q_2^{(0)} - 2D_0 D_1 q_2^{(1)} - D_1^2 q_2^{(0)} - 2D_0 D_2 q_2^{(0)} + 2c_9 q_1^{(0)} q_1^{(1)} + c_5 q_1^{(0)^2} q_2^{(0)} + c_{13} q_2^{(0)^3} \\
&\quad + 2c_{10} q_2^{(0)} q_2^{(1)} + c_2 q_1^{(1)} q_3^{(0)} + c_{12} q_1^{(0)} q_2^{(0)} q_3^{(0)} + c_{14} q_2^{(0)} q_3^{(0)^2} + c_2 q_1^{(0)} q_3^{(1)} + 2c_{11} q_3^{(0)} q_3^{(1)} \\
D_0^2 q_3^{(2)} + \omega_3^2 q_3^{(2)} &= -d_3 D_0 q_3^{(0)} - 2D_0 D_1 q_3^{(1)} - D_1^2 q_3^{(0)} - 2D_0 D_2 q_3^{(0)} + c_{16} q_1^{(0)^3} + c_2 q_1^{(1)} q_2^{(0)} + c_8 q_1^{(0)} q_2^{(0)^2} + c_2 q_1^{(0)} q_2^{(1)} \\
&\quad + c_6 q_1^{(0)^2} q_3^{(0)} + c_{14} q_2^{(1)^2} q_3^{(0)} + c_{15} q_2^{(1)} q_3^{(0)} + c_{18} q_1^{(0)} q_3^{(0)^2} + c_{17} q_3^{(0)^3} + c_{15} q_2^{(0)} q_3^{(1)} + c_{20} p e^{i\Omega T_0}
\end{aligned} \tag{17}$$

where  $D_i() = \partial()/\partial(T_i)$ ,  $D_{ij}() = \partial^2()/\partial(T_i)\partial(T_j)$  ( $i, j = 0, 1, 2$ ) and the tilde has been omitted for simplicity.

The solution to the first-order perturbation equations (15) is:

$$q_i^{(0)} = A_i(T_1, T_2) e^{i\omega_i T_0} + c.c. \quad i = 1, 2, 3. \tag{18}$$

where  $c.c.$  stands for the complex conjugate of the preceding terms and  $A_i$  are the unknown complex-valued functions. In order to investigate the system response under internal and external resonance conditions, three detuning parameters  $\sigma_i$  are introduced:

$$\Omega = \omega_1 + \varepsilon^2 \sigma_1, \quad \omega_2 = 2\omega_1 + \varepsilon \sigma_2, \quad \omega_3 = 3\omega_1 + \varepsilon^2 \sigma_3 \tag{19}$$

Solving the  $\varepsilon^2$ -order perturbation equations and then using a reconstitution method (Nayfeh, 1985), to return to true time  $t$ , and introducing a Cartesian coordinates (20), the following amplitude and phase equations (21) are finally obtained:

$$A_k = \frac{1}{2} (p_k - iq_k) e^{iv_k} \quad k = 1, 2, 3. \tag{20}$$

$$\begin{aligned}
p_1' &= -\frac{d_1 p_1}{2} - q_1 \sigma_1 - \frac{c_1 p_2 q_1 \sigma_2}{8\omega_1^2} + \frac{c_1 p_1 q_2 \sigma_2}{8\omega_1^2} + \frac{c_2 p_3 q_2 \sigma_2}{8\omega_1^2} - \frac{c_2 p_2 q_3 \sigma_2}{8\omega_1^2} - \frac{b_1 p_1^2 q_1}{8\omega_1} + \frac{c_1 p_2 q_1}{4\omega_1} - \frac{b_3 p_2^2 q_1}{8\omega_1} + \frac{b_2 p_1 p_3 q_1}{4\omega_1} - \frac{b_5 p_3^2 q_1}{8\omega_1} \\
&\quad - \frac{b_1 q_1^3}{8\omega_1} - \frac{c_1 p_1 q_2}{4\omega_1} + \frac{c_2 p_3 q_2}{4\omega_1} - \frac{b_4 p_2 p_3 q_2}{4\omega_1} - \frac{b_3 q_1 q_2^2}{8\omega_1} - \frac{b_2 p_1^2 q_3}{8\omega_1} - \frac{c_2 p_2 q_3}{4\omega_1} + \frac{b_4 p_2^2 q_3}{8\omega_1} + \frac{b_2 q_1^2 q_3}{8\omega_1} - \frac{b_4 q_2^2 q_3}{8\omega_1} - \frac{b_5 q_1 q_3^2}{8\omega_1} \\
p_2' &= -\frac{d_2 p_2}{2} - 2q_2 \sigma_1 - \frac{c_9 p_1 q_1 \sigma_2}{4\omega_2^2} + \frac{c_2 p_3 q_1 \sigma_2}{8\omega_2^2} + \frac{c_2 p_1 q_3 \sigma_2}{8\omega_2^2} - \frac{c_9 p_1 q_1}{2\omega_2} + \frac{c_2 p_3 q_1}{4\omega_2} - \frac{b_9 p_2 p_3 q_1}{8\omega_2} - \frac{b_6 p_1^2 q_2}{8\omega_2} - \frac{b_7 p_2^2 q_2}{8\omega_2} + \frac{b_9 p_1 p_3 q_2}{8\omega_2} \\
&\quad - \frac{b_8 p_3^2 q_2}{8\omega_2} - \frac{b_6 q_1^2 q_2}{8\omega_2} - \frac{b_7 q_2^3}{8\omega_2} - \frac{c_2 p_1 q_3}{4\omega_2} - \frac{b_9 p_1 p_2 q_3}{8\omega_2} - \frac{b_9 q_1 q_2 q_3}{8\omega_2} - \frac{b_8 q_2 q_3^2}{8\omega_2} \\
p_3' &= -\frac{d_3 p_3}{2} - 3q_3 \sigma_1 + q_3 \sigma_3 + \frac{c_2 p_2 q_1 \sigma_2}{8\omega_3^2} + \frac{c_2 p_1 q_2 \sigma_2}{8\omega_3^2} - \frac{3b_{10} p_1^2 q_1}{8\omega_3} - \frac{c_2 p_2 q_1}{4\omega_3} + \frac{b_{11} p_2^2 q_1}{8\omega_3} + \frac{b_{10} q_1^3}{8\omega_3} - \frac{c_2 p_1 q_2}{4\omega_3} - \frac{b_{11} p_1 p_2 q_2}{4\omega_3} \\
&\quad - \frac{b_{11} q_1 q_2^2}{8\omega_3} - \frac{b_{12} p_1^2 q_3}{8\omega_3} - \frac{b_{13} p_2^2 q_3}{8\omega_3} - \frac{b_{14} p_3^2 q_3}{8\omega_3} - \frac{b_{12} q_1^2 q_3}{8\omega_3} - \frac{b_{13} q_2^2 q_3}{8\omega_3} - \frac{b_{14} q_3^3}{8\omega_3} \\
q_1' &= -\frac{d_1 p_1}{2} - p_1 \sigma_1 - \frac{c_1 p_1 p_2 \sigma_2}{8\omega_1^2} + \frac{c_2 p_2 p_3 \sigma_2}{8\omega_1^2} - \frac{c_1 q_1 q_2 \sigma_2}{8\omega_1^2} + \frac{c_2 q_2 q_3 \sigma_2}{8\omega_1^2} + \frac{c_{19} p}{\omega_1} + \frac{b_1 p_1^3}{8\omega_1} + \frac{c_1 p_1 p_2}{4\omega_1} + \frac{b_3 p_1 p_2^2}{8\omega_1} + \frac{b_2 p_1^2 p_3}{8\omega_1} + \frac{c_2 p_2 p_3}{4\omega_1} \\
&\quad + \frac{b_4 p_2^2 p_3}{8\omega_1} - \frac{b_5 p_1 p_3^2}{8\omega_1} + \frac{b_1 p_1 q_1^2}{8\omega_1} - \frac{b_2 p_3 q_1^2}{8\omega_1} + \frac{c_1 q_1 q_2}{4\omega_1} + \frac{b_3 p_1 q_2^2}{8\omega_1} - \frac{b_4 p_3 q_2^2}{8\omega_1} + \frac{b_2 q_1 q_3}{4\omega_1} + \frac{c_2 q_2 q_3}{4\omega_1} + \frac{b_4 p_2 q_2 q_3}{4\omega_1} + \frac{b_5 p_1 q_3^2}{8\omega_1}
\end{aligned}$$

$$\begin{aligned}
 q_2' &= -\frac{d_2 q_2}{2} + 2p_2 \sigma_1 + \frac{c_9 p_1^2 \sigma_2}{8\omega_2^2} + \frac{c_2 p_1 p_3 \sigma_2}{8\omega_2^2} - \frac{c_9 q_1^2 \sigma_2}{8\omega_2^2} + \frac{c_2 q_1 q_3 \sigma_2}{8\omega_2^2} + \frac{c_9 p_1^2}{4\omega_2} + \frac{b_6 p_1^2 p_2}{8\omega_2} + \frac{b_7 p_2^3}{8\omega_2} + \frac{c_2 p_1 p_3}{4\omega_2} + \frac{b_9 p_1 p_2 p_3}{8\omega_2} \\
 &\quad + \frac{b_8 p_2 p_3^2}{8\omega_2} - \frac{c_9 q_1^2}{4\omega_2} + \frac{b_6 p_2 q_1^2}{8\omega_2} + \frac{b_9 p_3 q_1 q_2}{8\omega_2} + \frac{b_7 p_2 q_2^2}{8\omega_2} + \frac{c_2 q_1 q_3}{4\omega_2} - \frac{b_9 p_2 q_1 q_3}{8\omega_2} + \frac{b_9 p_1 q_2 q_3}{8\omega_2} + \frac{b_8 p_2 q_3^2}{8\omega_2} \\
 q_3' &= -\frac{d_3 q_3}{2} + 3p_3 \sigma_1 - p_3 \sigma_3 - \frac{c_2 p_1 p_2 \sigma_2}{8\omega_3^2} + \frac{c_2 q_1 q_2 \sigma_2}{8\omega_3^2} + \frac{b_{10} p_1^3}{8\omega_3} + \frac{c_2 p_1 p_2}{4\omega_3} + \frac{b_{11} p_1 p_2^2}{8\omega_3} + \frac{b_{12} p_1^2 p_3}{8\omega_3} + \frac{b_{13} p_2^2 p_3}{8\omega_3} + \frac{b_{14} p_3^3}{8\omega_3} \\
 &\quad - \frac{3b_{10} p_1 q_1^2}{8\omega_3} + \frac{b_{12} q_1^2 p_3}{8\omega_3} - \frac{c_2 q_1 q_2}{4\omega_3} + \frac{b_{11} p_2 q_1 q_2}{4\omega_3} - \frac{b_{11} p_1 q_2^2}{8\omega_3} + \frac{b_{13} q_2^2 p_3}{8\omega_3} + \frac{b_{14} p_3 q_3^2}{8\omega_3}
 \end{aligned} \tag{21}$$

where the prime indicates the derivative with respect to  $T_1$ .

## 6. NUMERICAL RESULTS

Non-linear coupling and resonant motions are investigated for a beam simply supported. In the numerical investigation the following geometrical and material characteristic are used:  $L = 6$  m,  $h = 0.6$  m,  $b = 0.6$  m,  $e = 0.03$  m. The analyzed material is graphite-epoxy whose properties are  $E_1 = 144$  GPa,  $E_2 = 9.65$  GPa,  $G_{12} = 4.14$  GPa,  $G_{13} = 4.14$  GPa,  $G_{23} = 3.45$  GPa,  $\nu_{12} = 0.3$ ,  $\nu_{13} = 0.3$ ,  $\nu_{23} = 0.5$ , for a sequence of lamination  $\{0/0/0/0\}$ . The solution of the linear free dynamic problem furnishes the following first three eigenvalues:

$$\omega_1 = 213.86 \text{ rad/s} \quad , \quad \omega_2 = 444.36 \text{ rad/s} \quad , \quad \omega_3 = 666.85 \text{ rad/s}.$$

The coefficients of the discretized equations of motion (13) are listed in Tab. 1.

Table 1. Coefficients of the non-dimensional discretized equations of motion.

$c_1$	$c_2$	$c_3$	$c_4$	$c_5$	$c_6$	$c_7$
23134.1	-38059.0	-12549.1	51358.0	-2057.39	-93052.5	58212.7
$c_8$	$c_9$	$c_{10}$	$c_{11}$	$c_{12}$	$c_{13}$	$c_{14}$
3375.58	11569.2	322.56	31345.8	6752.41	-0.61	0.0
$c_{15}$	$c_{16}$	$c_{17}$	$c_{18}$	$c_{19}$	$c_{20}$	
62660.6	19398.2	-87918.5	154026.0	-0.00517	-0.00651	

### 6.1. Steady-state motions and stability

The equilibrium solutions of Equations (21) correspond to periodic motions of the beam. Steady-state solutions are determined by zeroing  $p_i' = q_i' = 0$  the right-hand members of the modulation equations (21) and solving the non-linear system. Stability analysis is then performed by analyzing the eigenvalues of the Jacobian matrix of the non-linear equations calculated at the fixed points. Amplitude-load curves are reported in Fig. 3a and 3b, for external forces in a perfect resonance condition ( $\sigma_1 = 0$ ) and for a small value of the external detuning parameter  $\sigma_1 = 0.1$ , respectively, considering damping  $d_1 = d_2 = d_3 = 0.1$  and internal detuning parameters  $\sigma_2 = \sigma_3 = 0.04$ . The amplitudes  $a_1$ ,  $a_2$  and  $a_3$  are obtained by means of the following expression:

$$a_i = \sqrt{p_i^2 + q_i^2} \quad i = 1, 2, 3. \tag{22}$$

In the case of  $\sigma_1 = 0.1$  (Fig. 3b), the modal solution branch alternatively loses and regains stability due to the presence of some saddle-nodes and Hopf bifurcations. In spite of that only the amplitude  $a_1$  is presented in Fig. 3b, the same behavior is obtained for the other amplitudes.

The frequency-response curves are shown in Fig. 4a, b and c, for an internal and external resonance condition. The modal amplitude  $a_i$  curves are obtained in function of the external detuning parameter  $\sigma_1$ . In this case, the forcing amplitude is  $p = 250$ , modal damping  $d_1 = d_2 = d_3 = 0.1$  and internal detuning parameters  $\sigma_2 = \sigma_3 = 0.04$ . In this way, near to  $\sigma_1 = 0.1$  the dynamic behavior will be complex as can be observed from Fig. 3b. In the Fig. 4, solid (dotted) lines denote stable (unstable) equilibrium solutions and thin solid lines denote unstable foci.

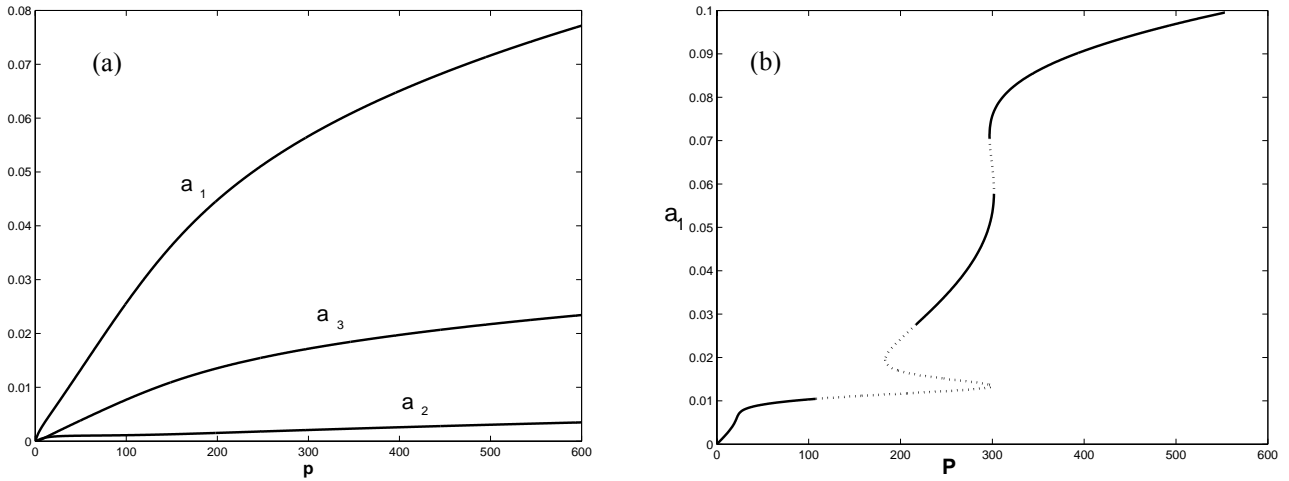


Figure 3. Amplitude-load curves: (a) Perfect external resonance  $\sigma_I = 0$ ; (b) External detuning parameter  $\sigma_I = 0.1$ . Thick line: stable solutions; dashed line: unstable solutions.

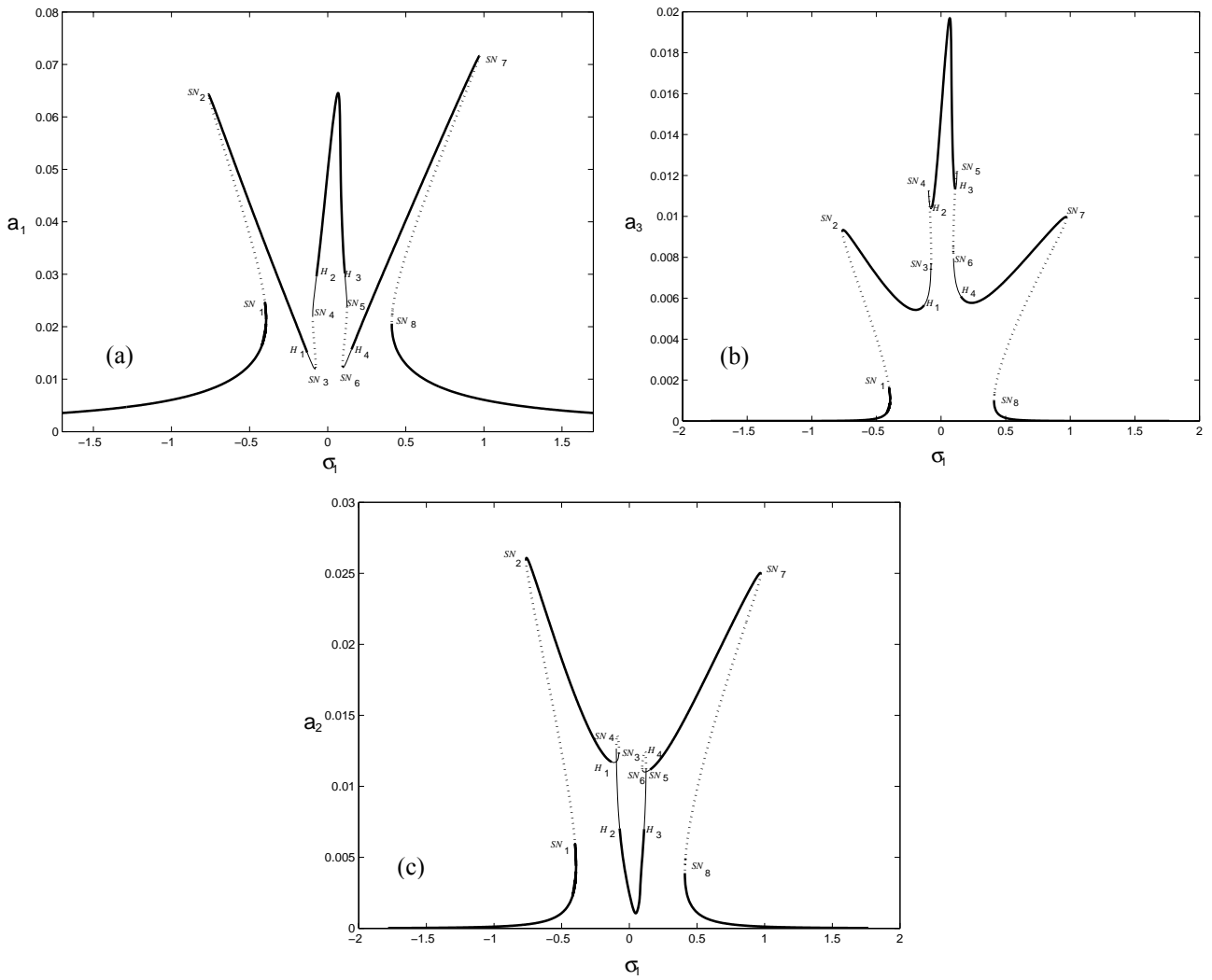


Figure 4. Frequency-response curves for: (a) first, (b) second and (c) third modes, when  $p = 250$ ,  $\sigma_2 = \sigma_3 = 0.04$  and  $d_i = 0.1$ . Solid (dotted) lines denote stable (unstable) equilibrium solutions and thin solid lines denote unstable foci.

The response curves exhibit a complex behavior due to saddle-node bifurcations (where one of the corresponding eigenvalues crosses the imaginary axis along the real axis from the left- to the right-half plane) and Hopf bifurcations

(where one pair of complex conjugate eigenvalues crosses the imaginary axis transversely from the left to the right-half plane). As  $\sigma_I$  increases from a small value, the solution increases in amplitude and is stable until a saddle-node bifurcation occurs  $\sigma_I = -0.3938$  ( $SN_1$ ). Then, the response jumps to another branches of stable equilibrium solutions (jump effect), depending on the initial conditions. Increasing  $\sigma_I$ , the amplitude decreases until the stable equilibrium solution loses stability via a Hopf bifurcation at  $H_1$  ( $\sigma_I = -0.1307$ ). Then, the solution is unstable happening two saddle-node bifurcations  $SN_3$  and  $SN_4$  ( $\sigma_I = -0.0763$  and  $\sigma_I = -0.0961$ ) and regains its stability via a reverse Hopf bifurcation at  $H_2$  ( $\sigma_I = -0.0724$ ). Then, an approximated symmetric solution is observed for  $\sigma_I$  larger than the perfect external resonant condition. Therefore, the solution loses stability via a Hopf bifurcation  $H_3$  ( $\sigma_I = 0.1094$ ), and regains its stability via a reverse Hopf bifurcation at  $H_4$  ( $\sigma_I = 0.1530$ ), happening two saddle-node bifurcations  $SN_5$  and  $SN_6$ , ( $\sigma_I = 0.1238$  and  $\sigma_I = 0.0946$ ). The stable solution grows again in amplitude until arriving to a saddle-node bifurcation  $SN_7$  ( $\sigma_I = 0.9718$ ), resulting in a jump of the response to another branches of solutions. The new stable branch is left bounded by a saddle-node bifurcation  $SN_8$  ( $\sigma_I = 0.4102$ ). On the other hand, comparing the three modal amplitude  $a_i$  curves, the highest values correspond to the first mode which is directly excited by the external load.

### 6.2. Dynamic solutions

According to the Hopf bifurcation theorem, small limit cycles are born as a result of the Hopf bifurcation. The born limit cycles are stable if the bifurcation is supercritical and unstable if the bifurcation is subcritical. Cycle-limit of the modulation equations correspond to aperiodic responses of the beam. In the previous example ( $d_3 = 0.1$ ,  $\sigma_2 = \sigma_3 = 0.04$  and  $p = 250$ ), there are four hopf bifurcations. Where  $H_1$  ( $\sigma_I = -0.1307$ ) and  $H_4$  ( $\sigma_I = 0.1530$ ) represent subcritical Hopf

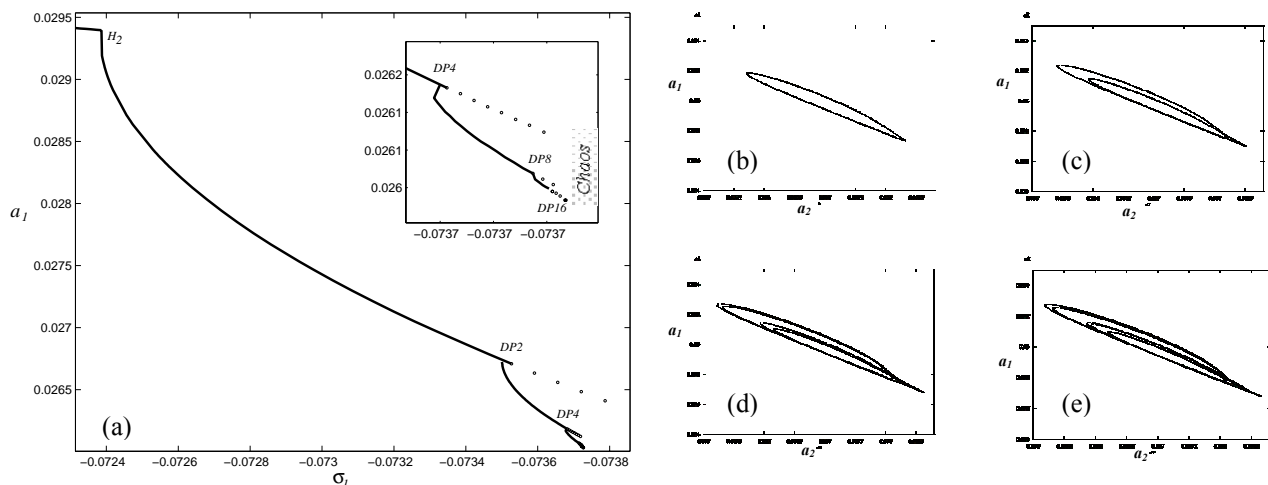


Figure 5. a) Schematic of the dynamic solutions found on one branch for the first mode. (—) Stable limit cycle, (o o o) unstable limit cycle,  $DP_n = n$ th period doubling bifurcation. Two-dimensional projections of the phase portraits onto the  $a_1$ - $a_2$  plane, b)  $\sigma_I = -0.0734455$ , c)  $\sigma_I = -0.07358$ , d)  $\sigma_I = -0.073695$ , e)  $\sigma_I = -0.073715$ .

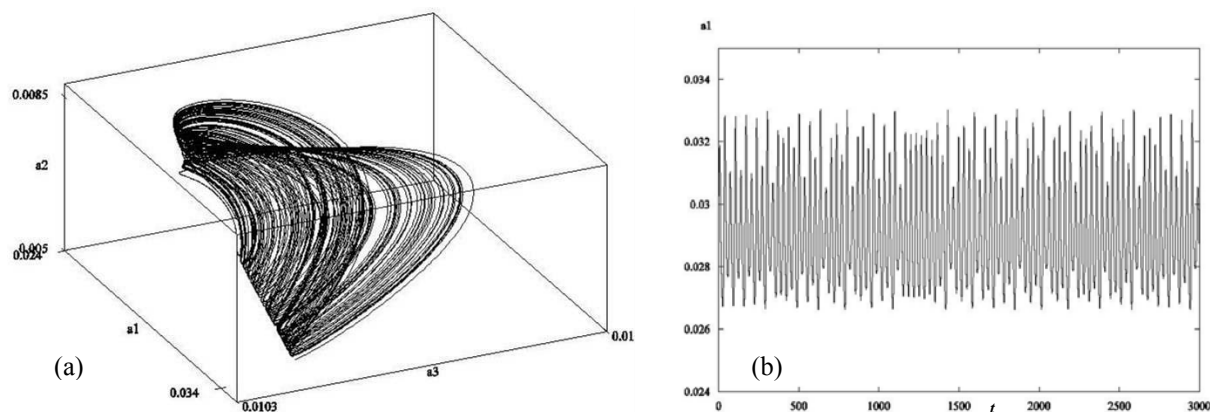


Figure 6. Attractor chaotic found at  $\sigma_I = -0.0737899$ . a) Three-dimensional projection of the phase portrait onto the  $a_1$ - $a_2$ - $a_3$  space, and (d) time history.

bifurcation, while  $H_2$  ( $\sigma_l = -0.0724$ ) and  $H_3$  ( $\sigma_l = 0.1094$ ) correspond to supercritical Hopf bifurcation. The software XPP-AUTO (Doedel, 1997) is used to obtain the dynamic solutions that emerge from  $H_2$ . As  $\sigma_l$  increases, a small limit cycle born as a result of the supercritical Hopf bifurcation point  $H_2$ , see Fig. 5a. The period-one limit cycle (Fig. 5b) grows and deforms and remains stable until another period-doubling bifurcation occurs  $DP2$  ( $\sigma_l = -0.07353$ ). Then it undergoes a sequence of period doubling bifurcations  $DP4$  ( $\sigma_l = -0.07368$ ),  $DP8$  ( $\sigma_l = -0.07371$ ),  $DP16$  ( $\sigma_l = -0.073721$ ), culminating in a chaotic attractor as shown in Fig. 6. In Figs. 5c-e, two-dimensional projections of the phase portraits onto the  $a_1$ - $a_2$  plane at various pre and post-period-doubling bifurcation points are shown.

## 7. CONCLUSIONS

In this paper a geometrically non-linear theory for thin-walled composite beams is presented. The theory is formulated in the context of large displacements and rotations, through the adoption of a second-order improved shear deformable displacement field (accounting for bending and warping shear). The theory accounts for bisymmetric cross-sections either open or closed. The response of a simply-supported beam under a vertical concentrated load to a primary resonant excitation of its first flexural-torsional mode is investigated. The frequency of the second and third mode is approximately two and three times that of the first mode and hence a two-to-one and three-to-one internal resonance can be activated. With the method of multiple scales six first-order nonlinear ordinary-differential equations describing the modulation of the amplitudes and phases were derived. The resonant behavior is illustrated by frequency-response and amplitude-load curves for a sequence of lamination of  $\{0/0/0/0\}$ . The frequency-response curves exhibit a complex behavior due to the presence of saddle-node and Hopf bifurcations. Supercritical and subcritical Hopf bifurcations of the tree-mode equilibrium solutions are found. The limit cycle solutions of the modulation equations may undergo a sequence of period-doubling bifurcations, culminating in chaos.

## 8. ACKNOWLEDGEMENTS

The present study was sponsored by Secretaría de Ciencia y Tecnología, Universidad Tecnológica Nacional, and by CONICET.

## 9. REFERENCES

- Barbero E., 1999, Introduction to Composite Material Design, Taylor and Francis Inc.
- Crespo da Silva, M. R. M. and Glynn, C. C., 1978a, "Nonlinear flexural-flexural-torsional dynamics of inextensional beams. I. Equations of motion", Journal of Structural Mechanics, Vol. 6, pp. 437-448.
- Crespo da Silva, M. R. M. and Glynn, C. C., 1978b, "Nonlinear flexural-flexural-torsional dynamics of inextensional beams. II. Forced motions", Journal of Structural Mechanics, Vol. 6, pp. 449-461.
- Crespo da Silva M.R.M., Zaretzky C.L., 1994, "Nonlinear flexural-flexural-torsional interactions in beams including the effect of torsional dynamics. I: Primary resonance", Nonlinear Dynamics, Vol. 5, pp. 3-23.
- Doedel E.J., 1997, "AUTO97 Continuation and bifurcation software for ordinary differential equations", Available by anonymous ftp from FTP.CS.CONCORDIA.CA, directory PUB/DOEDEL/AUTO.
- Luongo A., Rega G., Vestroni F., 1989, "Non resonant non-planar free motions of inextensional non-compact beams", Journal of Sound and Vibration, Vol. 134, pp. 73-86.
- Machado S.P., Cortinez V.H., 2005, "Non-Linear model for stability of thin walled composite beams with shear deformation", Thin walled Structures, Vol. 43, pp. 1615-1645.
- Nayfeh A.H., 1973, "Perturbation Methods", Pure & Applied Mathematics-A Wiley Interscience Series of Text, Monographs & Tracts, New York.
- Nayfeh, A.H. and Mook, D.T., 1979, "Nonlinear Oscillations", Wiley, New York.
- Nayfeh A.H., 1985, "Topical course on nonlinear dynamics, in: Perturbation Methods in Nonlinear Dynamics", Societua Italiana di Fisica, Santa Margherita di Pula, Sardinia.
- Nayfeh, A.H. and Balachandran B., 1989, "Modal interactions in dynamical and structural systems", Applied Mechanics Reviews, Vol. 42, pp. 175-201.
- Nayfeh, A.H., 1996, "Nonlinear Interactions", Wiley, New York.

## 10. RESPONSIBILITY NOTICE

The authors are the only responsible for the printed material included in this paper.